MULTI-MODE PIEZOELECTRIC MICROMACHINED TRANDUCERS FOR MULTI-CHANNEL ACOUSTIC POWER TRANSFER AND DATA TELEMETRY

Teng Zhang, Ashwin A. Seshia
Department of Engineering, University of Cambridge, Cambridge, UK

ABSTRACT

This paper reports on a piezoelectric micromachined ultrasonic transducer (PMUT) with a customized electrode design based on distinctive mode shapes, which enables a single transducer to realize acoustic power transfer and multi-channel data telemetry simultaneously. A prototype device is tested for concurrent 2-channel functionality in wireless power transfer and data telemetry for simultaneous transmission of carrier signals at frequencies of 101.45 kHz and 828 kHz corresponding to specific device modes. An output power transfer of 1.52 µW and data rate of 200 kbps is demonstrated across a pair of PMUT devices in air for a separation of 1 cm.

KEYWORDS

Piezoelectric micromachined ultrasonic transducer (PMUT), multi-frequency operation, wireless power transfer, data telemetry.

INTRODUCTION

Miniaturization in ultrasound transducers has seen significant progress with widespread application and continued research in materials and fabrication processes, design innovation and system integration. Piezoelectric micromachined ultrasound transducers (PMUTs) have particularly drawn significant interest in recent years in wide ranging applications such as ultrasonic ranging, haptic interfaces, medical imaging and fingerprint sensing [1, 2]. The vast majority of PMUT literature addresses fixed-frequency operation at or around a specific resonance mode (typically fundamental mode). The specific PMUT design, including the selection of the stack of materials, particular topologies and operating frequency is dictated by the application context.

Despite the very impressive advances in PMUT development, a gap in the literature exists with respect to exploring the ability of PMUTs to operate over multiple frequencies and over wide frequency ranges. Both features can significantly augment PMUT capabilities. For instance, previous related work in this area includes research on PMUT arrays comprising elements operating at different frequencies for imaging applications. Wang *et al.* and Cai *et al.* proposed PMUT arrays incorporating transducers with different dimensions and consequently different operating frequencies [3, 4]. These designs are however limited by the number of transducers operating at a particular frequency due to the trade-off between the number of devices of a particular design that can accommodated in a limited chip area [5]. On the other hand, multi-mode operation has been explored in the context of other MEMS devices, offering an opportunity to operate at multiple frequencies in a single device structure [6, 7]. This can be extended to PMUTs where electrode shaping can provide selective access to multiple modes within a single device. Both fundamental and higher-order modes can be simultaneously interrogated with the proposed designs addressing the multi-frequency aspect discussed above but without sacrificing array element density.

In this study, multi-mode operation of PMUTs is explored to enable both low- and high- frequency ultrasound links between two individual PMUTs for acoustic power transfer and data telemetry applications. Such multi-channel PMUTs can enable enhanced acoustic power transfer and increased bandwidth data telemetry at low error rates. Intended applications include biomedical implants where an integrated PMUT array could be operated in a multi-channel configuration with a low-frequency carrier providing acoustic power transfer for deep-tissue biomedical implants while simultaneously utilizing one or more high frequency channels for acoustic data telemetry.

DEVICE DESIGN

An AlN-on-SOI fabrication platform is adopted for PMUT manufacturing. The device utilizes a piezoelectric MEMS process employing a 0.5 µm aluminum nitride (AlN) thin film deposited on a 10 µm doped silicon device layer. The cross-sectional view of the device is shown in Figure 1(A). The 10 µm doped silicon device layer serves as the bottom electrode and the top electrode is formed from a metal layer composed of 20 nm of Cr and 1000 nm of Al. In addition, a customized dual-electrode layout is proposed based on the mode shape of the fundamental and higher order modes. The design is shown in Figure 1 and features a circular PMUT with a radius of 660 µm and a fundamental (0,1) mode at approximately 100 kHz. To achieve maximal electromechanical coupling efficiency for this mode, a central circular electrode covers 60% of the membrane area.

Higher-order modes were also recorded by electrically driving the PMUT over a frequency range up to 1 MHz and recording the response using a digital holographic microscope (DHM). Figures 2 and 3 show sweep frequency responses and representative recorded optical spectrum for a driving voltage amplitude of 10 V peak-to-peak. Notably, the higher order modes, especially the (0, 2) and (0, 3) modes, exhibit a strong and distinctive deflection pattern in the borderline area in contrast to the (0,1) mode. A second annular electrode was integrated onto the periphery of the PMUT at a 10 µm gap spacing away from the central circular electrode to provide channel select functionality. Each electrode can select for a response at a designated frequency channel, and this approach can be extended in principle for other high-order modes. The experimental data demonstrates a significant selection advantage by electrode design enabling isolation of high- and low- frequency signals from different recording locations when the PMUT is simultaneously driven in more than one mode [8-10].

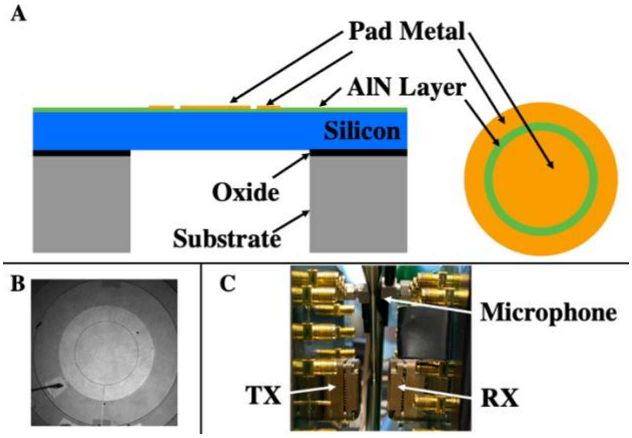

Figure 1: A: Cross-Sectional View of AlN-on-SOI topology illustrating a design consisting of two electrodes. B: Fabricated PMUT as viewed under a DHM. C: Experimental setup with one PMUT as TX (transmitter) and another as RX (receiver) in air.

Overall, the proposed PMUT design and electrode layout provide effective means to optimize electromechanical coupling efficiency and channel selectivity for different modes, enabling a more versatile and robust device for a range of potential applications.

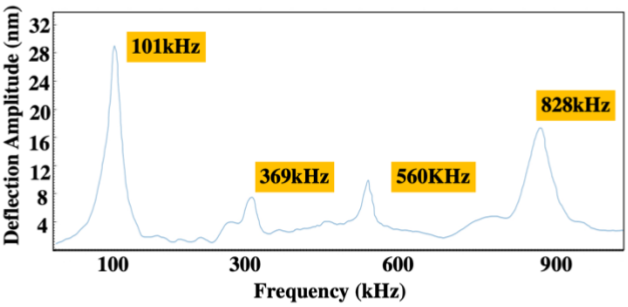

Figure 2: Optically measured frequency response of the PMUT showing 4 distinctive modes under 1MHz.

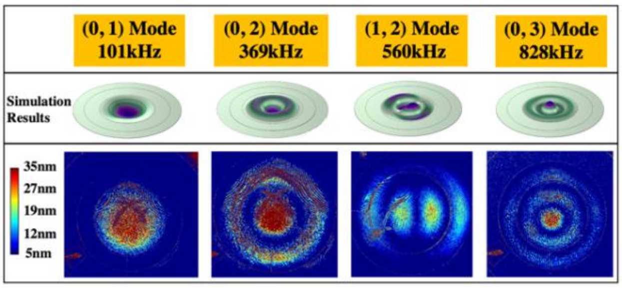

Figure 3: Mode shapes and maximal deflection amplitude corresponding to each mode under 10V pk-to-pk. The middle row shows simulated mode shapes, and the bottom row is the DHM recorded vibration profiles.

DEVICE CHARACTERIZATION

In the experimental setup, a pair of PMUTs is integrated into a custom jig that enables precise control of the spacing between them in an air medium. The measurements are conducted with one of the PMUTs acting as a transmitter (TX) and the other as a receiver (RX) with testing carried out for both single- and multi-channel response. The transmitter is firstly driven in the (0,1) mode and the receiver's electrical response is recorded from the inner electrodes. Figure 4 illustrates the open-circuit output voltage of the receiver as a function of separation distance under a 10 V pk-to-pk and 101 kHz AC drive. As the separation distance increases, the output voltage amplitude drops exponentially, and the output voltage then steadily reduces. This trend is similarly observed for the higher order modes, and therefore, the 10 mm separation distance is chosen for the experiments.

For single channel operation, a calibrated microphone is inserted between TX and RX to keep records of ultrasound intensity in air. The PMUT impedance is measured to be 3000 Ω, and for acoustic power transfer experiments, a matched external load resistor is employed at the receiving PMUT. When driving the PMUT transmitter with 10 V pk-to-pk continuous signal at its fundamental mode, the experiments reveal that a single PMUT receiver response records a maximal 67.53 mV output voltage amplitude, equivalent to power transfer of 1.52 µW to the load resistor at 1 cm distance. This result corresponds to an transmit ultrasound power intensity of 0.18 mW/cm^2, well below the FDA ultrasound safety limit of 720 mW/cm^2 [11-13].

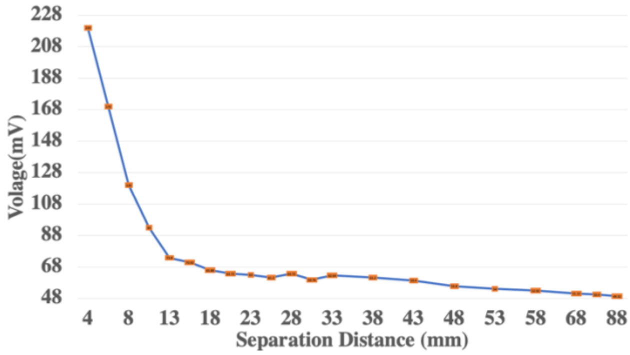

Figure 4: Open-circuit voltage recorded at the receiver in the (0,1) mode as a function of separation distance between the transmitter and receiver.

In the context of experimental results pertaining to the multi-mode PMUT when operated in the dual-channel mode, a complex driving signal is utilized by combining carrier signals at both (0,1) and (0,3) natural frequencies. The resulting waveform is illustrated in figure 5. Since both targeted modes are symmetric, two points of interest were carefully selected to distinguish the vibration profiles based on their unique deflection characteristics. Specifically, the center of the center electrode (point A) was chosen to evaluate the flexural response of the fundamental (0,1) mode, while point B was selected to observe the vertical deflection amplitude of the (0,3) mode, which arises due to the unique stress distribution across the annular electrode. The results indicate that despite both modes exhibiting a strong deflection pattern at point A, the fundamental (0,1) mode yields a much stronger and dominant response in that region. Similarly, the frequency response from the outer annular electrode at point B shows good mode selection, with its output primarily dominated by the 828 kHz signal and minimal interference from the lower frequency mode.

Furthermore, the observed results are supported by the measured electrical response. These findings provide valuable insight into the behavior of multi-mode PMUTs when driven by complex waveforms and demonstrate the potential for exciting multiple modes simultaneously for enhanced functionality.

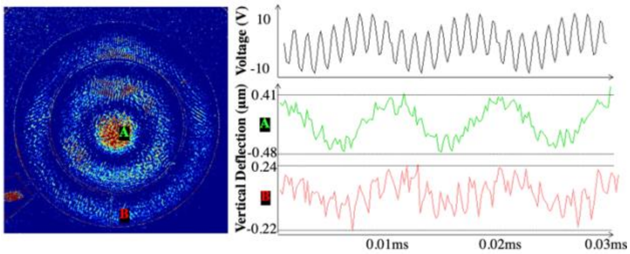

Figure 5: Deflection profile (left) of the PMUT measured under a DHM when driven by a summed signal (top right) and measurement results (right middle and bottom rows) of points A and B at the middle of the center and annular electrodes. The annular electrode at point B exhibits distinct vibration characteristics, with more pronounced features at higher frequencies that correspond to the (0,3) mode.

MULTI-MODE WPT AND COM LINKS

The previous section demonstrated the simultaneous excitation of multiple modes in PMUTs offering the potential for enhancing functionality. One of the advantages of multi-mode PMUTs is their ability for simultaneous and independent manipulation of acoustic waves in different frequency ranges. To explore this potential, a concurrent Wireless Power Transfer (WPT) and Communication (COM) links concept is introduced in the context of a dual-channel PMUT. Such a demonstration could motivate future applications that leverage the ability of lower frequency ultrasound for more efficient acoustic power transfer over longer distances while employing high-frequency ultrasound for increased data transfer rate in the context of wireless communication.

In order to ensure efficient and reliable data transfer, it is essential to carefully select the carrier signal frequency for the communication (COM) channel and optimize it for the wireless power transfer (WPT) channels. Through our experimental studies, we have discovered that an effective way to limit the Bit Error Rate (BER) in data transfer is to choose a carrier frequency that is an integer or nearly integer multiple corresponding to even multiples of the WPT channel frequency. This approach reduces signal interference on each bit when the WPT signal transits from one half period to the next, especially when two signals with distinct frequencies are mixed. Additionally, the communication resolution is dependent on the acoustic intensity, which is directly related to the vibration amplitude of the PMUT. Therefore, selecting the appropriate mode and its associated vibration amplitude is critical for achieving optimal communication performance.

In this study, we chose the (0,3) mode as the COM channel and used modulation to explore the PMUT's communication capabilities. Specifically, we introduced a binary signal with a bit duration of 0.5 µs and modulated the carrier signal of 828 kHz using the amplitude-shift keying (ASK) protocol. For simultaneous acoustic power transfer, we targeted the (0,1) mode, and the transmitter was fed with a continuous sinusoidal signal at a resonance frequency of 101 kHz. By employing these techniques, we were able to achieve effective and efficient communication and power transfer using the PMUTs.

As shown in Figure 6, the transmitter PMUT was driven with a combined signal, and the green waveform represents the COM channel encoded with the binary signal, while the red waveform shows the acoustic power transfer that is simultaneously fed to the transmitting PMUT. While the transmitting PMUT was driven with a combined signal, two electrodes on the receiving PMUT were targeted to collect and isolate signals from the two separate channels. The inner electrode received a continuous WPT signal, while the annular electrode on the PMUT receiver picked up the transmitted COM signal. The electrical output in the middle of Figure 6 demonstrates minimal interference from the low frequency mode. The data was demodulated at the receiving end, resulting in an equivalent data transfer rate of 200 kbps and a low bit error rate (BER) of 9.7×10^{-4}, demonstrating the dual/multi- channel PMUT's communication capability.

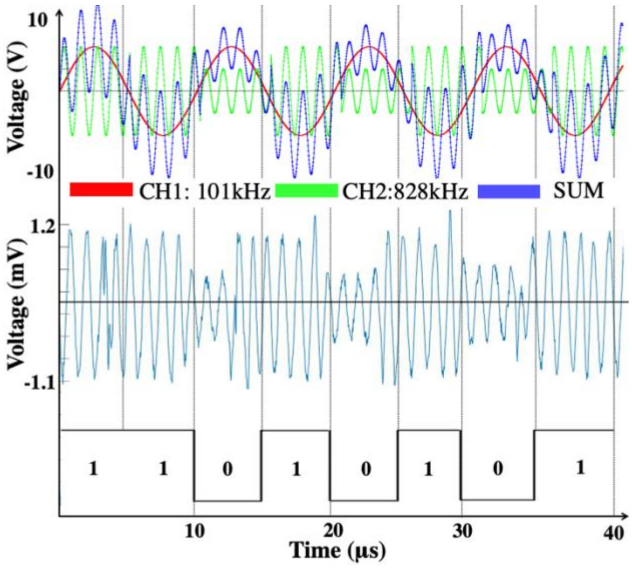

Figure 6. Top row: driving signal (blue) with binary data encoded at channel 2. Middle row: open-circuit voltage output from the annular electrode. Bottom row: demodulated binary signal.

Since the vibration amplitude and signal intensity is weaker for higher frequency and higher modes, the driving level for each channel can be adjusted to compensate for this effect [5]. For instance, since the natural frequency response at the wireless power transfer (WPT) channel is twice that of the communication (COM) channel, reducing the peak-to-peak drive level for the WPT from 10 V to 2.5 V can help sustain high resolution on the communication channel while still achieving effective power transfer. Despite a low BER, this approach resulted in a significant reduction in transferred power, from 1.52 μW to 31.3 nW. On the other hand, if power efficiency is a priority for a given application, maintaining the drive level at 10 V for both channels could yield 1.28 μW of power, but at the expense of a higher bit BER, which then increases from 9.7×10^{-4} to 2.3×10^{-2}. Therefore, finding the appropriate balance in the driving levels at the two frequencies is essential to optimize the performance of PMUT devices that provide simultaneous power transfer and communication functionalities.

CONCLUSION

In summary, the proposed PMUT design demonstrates the ability to operate simultaneously in multiple modes, enabling concurrent wireless power transfer and communication functions. The results of our tests show that by appropriately selecting the modes of operation, it is possible to achieve both high data transfer rates and low bit error rates while wirelessly transferring power to a second receiving device. These capabilities could be of significant importance in the development of miniature devices for biomedical and other applications.

For instance, modern implantable medical electronics require low power consumption, with devices such as cardiac pacemakers and biosensors operating with power consumption levels measured in the few microwatts to hundreds of microwatts. Despite the relatively low transmitting sensitivity of AlN-PMUT, our results show that the transferred power reaches up to 1.52 μW and 31.3 nW for single- and multi-channel operations, respectively, under an acoustic transmission intensity of 0.28 mW/cm^2, which is less than 0.1% of the FDA ultrasound threshold of 720 mW/cm^2 [11-13]. It is worth noting that the optimal performance of the communication channel was prioritized in our design, which led to the lower power output. However, if power efficiency is the primary concern, maintaining a high drive level for both channels could still yield a 1.28 μW power output under multi-mode operation. On the other hand, while the fundamental mode and its low frequency benefits wireless power transmission, the concurrent high frequency COM channel enables higher data transfer rates relative to a lower frequency single channel. The performance is expected to be further improved in an application environment with better acoustic matching to the medium between the PMUTs.

Overall, the results of our study provide evidence of the potential for enabling simultaneous acoustic wireless power transfer and communication functionality using a pair of PMUTs. Future work can address the integration of a high-density PMUT array and the use of a high- sensitivity ultrasound transmitter to increase the overall power output and improve communication resolution for further miniaturization in the context of medical implants and other applications.

REFERENCES

[1] F. Pop, B. Herrera, and M. Rinaldi, "Lithium Niobate Piezoelectric Micromachined Ultrasonic Transducers for high data-rate intrabody communication," *Nature communications*, vol. 13, no. 1, pp. 1-12, 2022.

[2] S. Pala, Z. Shao, Y. Peng, and L. Lin, "Ultrasond-induced haptic sensations via PMUTS," in *2021 IEEE 34th International Conference on Micro Electro Mechanical Systems (MEMS)*, 2021: IEEE, pp. 911-914.

[3] H. Wang, H. Yang, H. Jiang, Z. Chen, P. X.-L. Feng, and H. Xie, "A multi-frequency PMUT array based on ceramic PZT for endoscopic photoacoustic imaging," in *2021 21st International Conference on Solid-State Sensors, Actuators and Microsystems (Transducers)*, 2021: IEEE, pp. 30-33.

[4] J. Cai *et al.*, "Beyond fundamental resonance mode: high-order multi-band ALN PMUT for in vivo photoacoustic imaging," *Microsystems & Nanoengineering*, vol. 8, no. 1, p. 116, 2022.

[5] J. A. Balasingam, S. Swaminathan, and A. Emadi, "A Low-Frequency Piezoelectric Micromachined Ultrasonic Transducer based on Multi-User MEMS Process with Enhanced Output Pressure," in *2020 IEEE International Ultrasonics Symposium (IUS)*, 2020: IEEE, pp. 1-4.

[6] A. Ganesan and A. Seshia, "A Proposal for Absolute Inertial Imaging using Two Mechanical Modes," in *2018 IEEE International Frequency Control Symposium (IFCS)*, 2018: IEEE, pp. 1-5.

[7] H. Zhang *et al.*, "A low-noise high-order mode-localized MEMS accelerometer," *Journal of Microelectromechanical Systems*, vol. 30, no. 2, pp. 178-180, 2021.

[8] J. S. Pulskamp *et al.*, "Electrode-shaping for the excitation and detection of permitted arbitrary modes in arbitrary geometries in piezoelectric resonators," *IEEE transactions on ultrasonics, ferroelectrics, and frequency control*, vol. 59, no. 5, pp. 1043-1060, 2012.

[9] L. Wu, X. Chen, G. Wang, and Q. Zhou, "Dual-frequency piezoelectric micromachined ultrasonic transducers," *Applied Physics Letters*, vol. 115, no. 2, p. 023501, 2019.

[10] T. Wang and C. Lee, "Electrically switchable multi-frequency piezoelectric micromachined ultrasonic transducer (pMUT)," in *2016 IEEE 29th International Conference on Micro Electro Mechanical Systems (MEMS)*, 2016: IEEE, pp. 1106-1109.

[11] T. R. Nelson, J. B. Fowlkes, J. S. Abramowicz, and C. C. Church, "Ultrasound biosafety considerations for the practicing sonographer and sonologist," 2009.

[12] US Department of Health and Human Services, Food and Drug Administration, Center for Devices and Radiological Health. (2019). "Marketing Clearance of Diagnostic Ultrasound Systems and Transducers." [Online] Available: https://www.fda.gov/media/71100/download

[13] L. Jiang, Y. Yang, Y. Chen, and Q. Zhou, "Ultrasound-induced wireless energy harvesting: From materials strategies to functional applications," *Nano Energy*, vol. 77, p. 105131, 2020.

CONTACTS

*T. Zhang, tel+44-07765002294; tz330@cam.ac.uk